

## Research Article

# Photoacoustic Measurement of Ethane with Near-Infrared DFB Diode Laser

Gang Cheng,<sup>1,2,3</sup> Yuan Cao,<sup>1,2</sup> Kun Liu ,<sup>1</sup> Gongdong Zhu,<sup>1</sup> Guishi Wang,<sup>1</sup> and Xiaoming Gao<sup>1</sup>

<sup>1</sup>Anhui Institute of Optics and Fine Mechanics, Chinese Academy of Sciences, Hefei 230031, China

<sup>2</sup>University of Science and Technology of China, Hefei 230031, China

<sup>3</sup>Anhui University of Science and Technology, Huainan 232001, China

Correspondence should be addressed to Kun Liu; liukun@aiofm.ac.cn

Received 27 February 2018; Accepted 17 April 2018; Published 9 May 2018

Academic Editor: Angelo Sampaolo

Copyright © 2018 Gang Cheng et al. This is an open access article distributed under the Creative Commons Attribution License, which permits unrestricted use, distribution, and reproduction in any medium, provided the original work is properly cited.

A compact resonant photoacoustic sensor based on a near-infrared distributed-feedback (DFB) diode laser was developed for detection of ethane ( $C_2H_6$ ). A DFB laser emission at  $5937.25\text{ cm}^{-1}$  with a power of  $\sim 5\text{ mW}$  was used as an excitation light source for generating the photoacoustic signal. Wavelength modulation and second harmonic detection scheme were employed. Modulation frequency and modulation amplitude were optimized for getting optimum performance. Performance evaluation based on the linearity response of the PAS sensor system with respect to  $C_2H_6$  concentration levels was performed, and a good linear dependence of the PAS signal on the  $C_2H_6$  concentration was obtained. A minimum detectable concentration of 9 ppmv was achieved for detection of  $C_2H_6$  with a lock-in time constant of 10 ms.

## 1. Introduction

Ethane ( $C_2H_6$ ) is the second largest component among natural gases; therefore, detection of  $C_2H_6$  was an effective method for discrimination of  $CH_4$  leakage between natural gas pipe line and biogenic sources of landfills or wetlands. Detection of  $C_2H_6$  is also important in environmental or atmosphere monitoring as  $C_2H_6$  strongly affects both atmosphere chemistry and climate as a most abundant nonmethane hydrocarbon in the atmosphere [1]. In addition,  $C_2H_6$  detection has found applications in breath analysis as a noninvasive method to monitor and identify diseases, such as lung cancer and asthma [2]. Therefore, developing the  $C_2H_6$  sensor has a strong need in industrial, environmental, or medical applications.

Laser spectroscopy-based gas sensors is an effective tool for real time, selective, and sensitive detection of trace gases, which has a wide range of potential applications in environmental monitoring, medical diagnostics, and industrial process control [3, 4]. Photoacoustic spectroscopy, based on the photoacoustic effect which was first discovered by

Alexander Graham Bell in 1880 [5], is a sensitive, selective, and well-established method for sensing trace gases that has been successfully employed in numerous applications [6, 7]. The PAS technique offers several practically important advantages, such as high trace gas detection sensitivity with a small sensing module and wide dynamic range and no need for an optical detector such as a photodiode. Unlike spectroscopic techniques, such as integrated cavity output spectroscopy (ICOS) [8], cavity ring down spectroscopy [9], or absorption spectroscopy with multipass cell [10], the PAS is a “zero base line” method. In addition, the amplitude of the photoacoustic signal depends on the power of the exciting light beam. Therefore, the PAS can benefit from using continuous wave infrared laser sources capable of emitting high optical power [11]. To date, there are several PAS techniques including traditional resonant PAS with wide-band microphones [12], cantilever-based PAS [13], and quartz-enhanced PAS (QEPAS) [14].

In the present work, we report on our recent efforts in the development of a compact PAS sensor for detection of  $C_2H_6$  by using a distributed-feedback (DFB) diode laser operating at

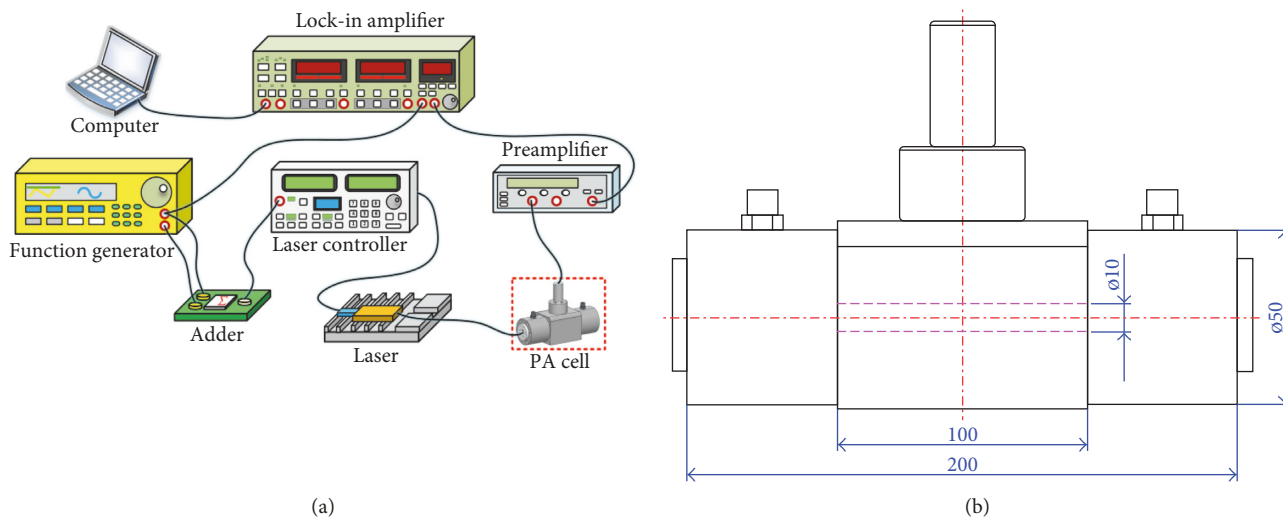


FIGURE 1: (a) Schematic diagram of the developed  $C_2H_6$  PAS experimental setup and (b) geometric dimension of the PAS cell.

$5937.2\text{ cm}^{-1}$  with a power of  $\sim 5\text{ mW}$  and an excitation light source to generate the photoacoustic signal. The near-infrared DFB diode lasers that are commercially available offer a robust, relatively inexpensive, and attractive alternative. This low-cost, compact, and sensitive PAS sensor of  $C_2H_6$  is very suitable for various field applications, in particular, for discrimination of  $CH_4$  leakage between natural gas pipe line and biogenic sources of landfills or wetlands [15].

## 2. $C_2H_6$ PAS Sensor Configuration

A schematic diagram of the developed  $C_2H_6$  PAS sensor platform is shown in Figure 1(a). A PAS cell built out of aluminum with a central cylinder tube of radius  $r = 5\text{ mm}$  and length of  $L = 100\text{ mm}$  acting as an acoustic resonator was designed. A buffer volume with a radius of  $25\text{ mm}$  and length of  $50\text{ mm}$  was set at both sides of the cylinder resonator, and the total length of the PAS cell was  $200\text{ mm}$  (Figure 1(b)).  $C_2H_6$  shows an unresolvable vibration-rotation absorption band near  $1.68\text{ }\mu\text{m}$  [16, 17]. Therefore, a fiber-coupled distributed-feedback (DFB) diode laser (NLK1E5GAAA, NEL) operating at  $1.684\text{ }\mu\text{m}$  was used as the excitation light source for generating the photoacoustic signal. The laser current and temperature were controlled by a commercial diode laser controller (ILX Lightwave LDC-3724). Coarse and fine wavelength tuning was performed by changing the laser temperature and current, respectively. Wavelength modulation and second harmonic detection are used in this work. A dual channel function generator was used to provide a voltage ramp for scanning the laser wavelength and a sine wave for modulating the laser wavelength. The voltage ramp and the sine wave were combined with a home-made adder before being fed to the laser driver. The laser current was the sine wave modulated at half the resonant frequency  $f_0$  of the PAS cell. The laser beam was collimated with a fiber-coupled collimator ( $f \sim 4.8\text{ mm}$ ) and subsequently focused into the PAS cell by using a lens L with a  $30\text{ mm}$  focal length. A preamplifier (EG&G, Model 5113) with a gain of 25 and 6 dB bandpass filter (300 Hz–30 kHz) was used for signal

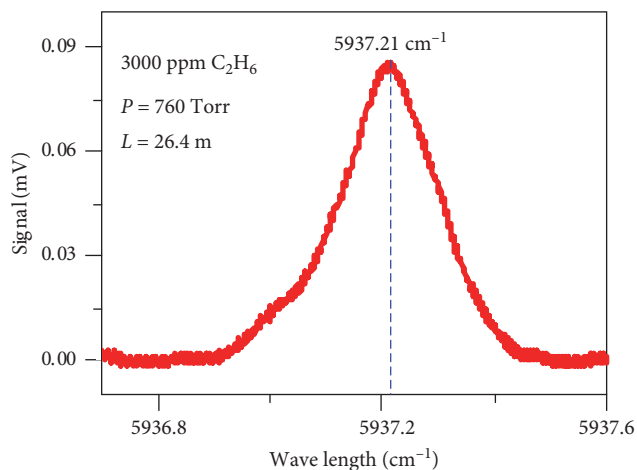


FIGURE 2: Direct absorption spectroscopy of  $C_2H_6$ .

amplification prior to demodulation at  $f_0$  by a lock-in amplifier (Stanford Research Systems, Model SR 830 DSP). The time constant of the lock-in amplifier was set at  $10\text{ ms}$  in combination with an  $18\text{ dB/octave}$  slope filter (leading to a detection bandwidth of  $\Delta f = 9.375\text{ Hz}$ ). The demodulated signal was subsequently digitalized with a DAQ card (NI-USB-6212) and displayed on a laptop via a LabVIEW interface.

## 3. Results and Discussion

Direct absorption spectroscopy of  $C_2H_6$  was first measured for determining absorption peak. Figure 2 shows a  $3000\text{ ppm}$   $C_2H_6$  absorption spectroscopy that was measured by using a compact multipass absorption cell with an optical path length of  $26.4\text{ m}$  [10] at normal atmosphere pressure. The absorption peak was found to be at  $5937.21\text{ cm}^{-1}$  and the corresponding laser temperature was  $31^\circ\text{C}$ . Therefore, the laser temperature was controlled at  $31^\circ\text{C}$  during following measurement.

Characteristics of the acoustic resonator were experimentally investigated to determine the specific resonant

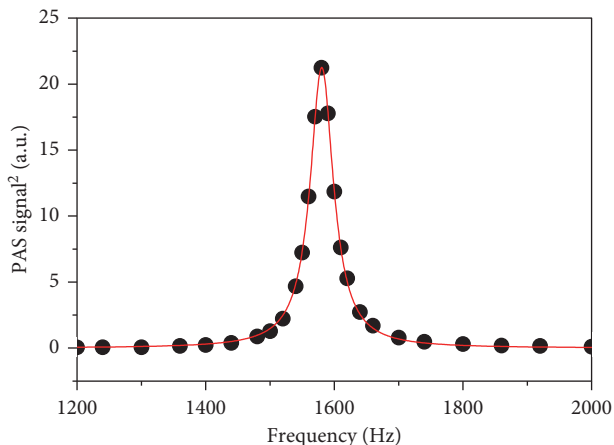


FIGURE 3: Square of the PAS signals amplitude as a function of frequency. The data are fitted with a Lorentz profile.

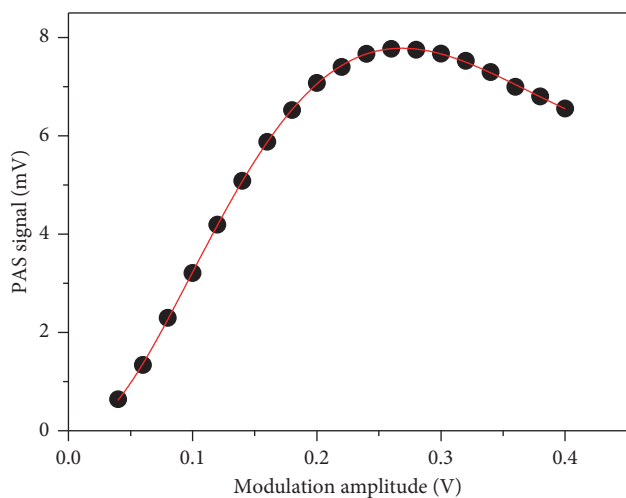


FIGURE 4:  $C_2H_6$  PAS signals as a function of modulation amplitude.

frequency of the resonator in an atmospheric environment. Measurements of the  $C_2H_6$  PAS signal with constant concentration of 5000 ppm at different modulation frequencies were performed for this study. Figure 3 shows the square of the signal amplitude as a function of frequency. The data were fitted to a Lorentz contour, which describes power in a classical driven oscillator as a function of frequency. From the results shown in Figure 3, optimum resonant frequencies  $f_{10} = 1580$  Hz were found for the resonator. This value corresponds to the first longitudinal resonant mode of the resonator [18]. Therefore, the laser wavelength was modulated at a frequency of 790 Hz.

The  $C_2H_6$  PAS sensor system was designed to operate in a wavelength modulation mode, which can effectively suppress the background noise. However, wavelength modulation of the PAS signal is dependent on modulation amplitude. Therefore, the laser frequency modulation amplitude was also to be optimized to get an optimum PAS signal. Figure 4 shows the measured PAS signal as a function of the modulation amplitude. The measurements were carried out under normal atmospheric conditions. As can be seen in Figure 4, the

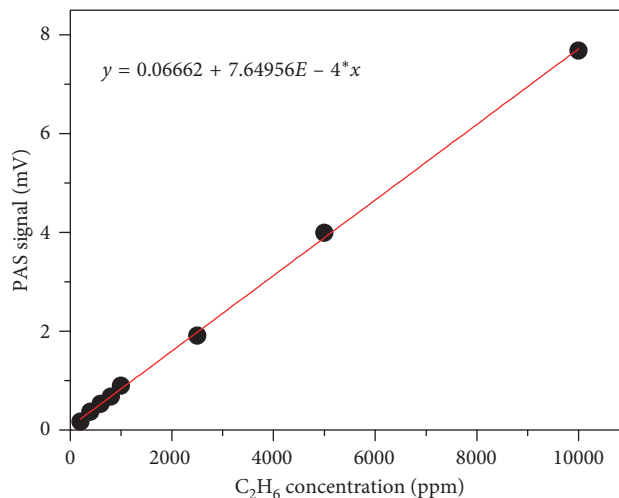


FIGURE 5: Linear response of the PAS signals to  $C_2H_6$  concentration.

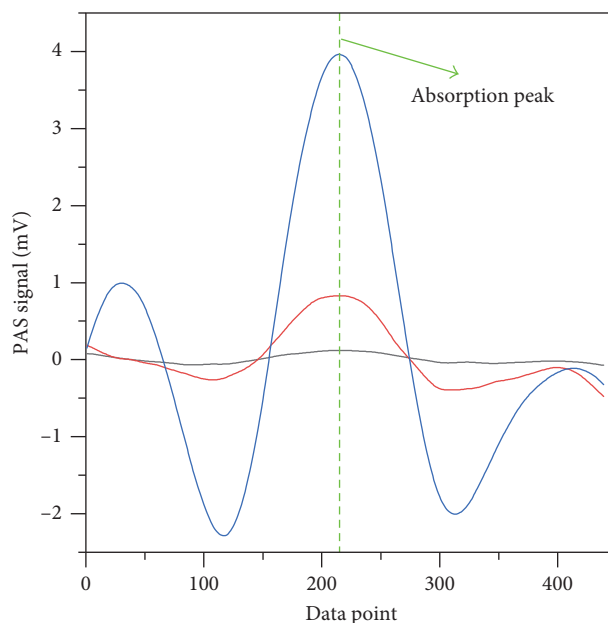


FIGURE 6:  $C_2H_6$  PAS signals obtained with 100 ppmv, 1000 ppmv, and 5000 ppmv  $C_2H_6$  samples, respectively. The dotted line position corresponds to the absorption peak of Figure 2.

optimum modulation amplitude of the sine wave for PAS detection of  $C_2H_6$  was found to be 0.25 V which was then used in the following measurements.

A performance evaluation based on the linearity response with optimized parameters of the  $C_2H_6$  PAS sensor system with respect to  $C_2H_6$  concentration levels was performed. A calibrated standard gas mixture consisting of 10,000 ppm  $C_2H_6:N_2$  was employed and diluted with pure  $N_2$  by using a commercial gas dilution system (EnviroNics, S4000). As expected, a linear dependence of the PAS signal on the  $C_2H_6$  concentration was found. The measured PAS signals and the fitted straight line are shown in Figure 5.

As an example, Figure 6 depicts the PAS  $2f$ -signals of  $C_2H_6$  with a concentration of 100 ppmv, 1000 ppmv, and

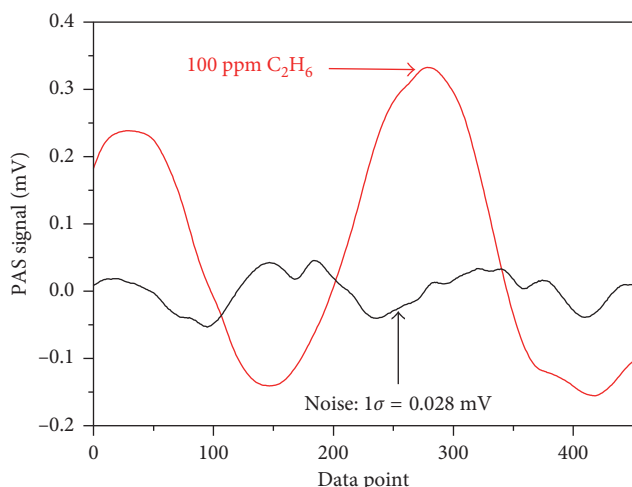


FIGURE 7: PAS signal of 100 ppmv  $C_2H_6$  and noise obtained in air.

5000 ppmv, respectively. The corresponding signal (the peak value at the dotted line) was 0.12 mV, 0.83 mV, and 3.96 mV, respectively. For evaluation of the minimum detection limit of the  $C_2H_6$  PAS sensor, the PAS signal in air, as the noise level, was measured. Figure 7 shows the PAS noise obtained in air and the 100 ppmv  $C_2H_6$  PAS signal for comparison. The noise level ( $1\sigma$ ) defined as standard deviation was found to be 0.028 mV. Taking into account the PAS signal of 0.33 mV obtained with 100 ppmv  $C_2H_6$ , the signal to noise ratio was then found to be 11. Therefore, the minimum detection limit was estimated to be 9 ppmv for  $C_2H_6$  detection.

#### 4. Conclusion

A PAS sensor for detection of  $C_2H_6$  was developed. Using wavelength modulation and second harmonic detection scheme, combined with optimization of modulation frequency and modulation amplitude, good performance was achieved for detection of  $C_2H_6$ . Good linear dependence of the PAS signal on the  $C_2H_6$  concentration was obtained. A minimum detectable concentration of 9 ppmv was achieved for detection of  $C_2H_6$  with a lock-in time constant of 10 ms and optical power of 5 mW. The developed  $C_2H_6$  PAS sensor could be applied in monitoring the natural gas pipe line leakage or industrial process control.

#### Data Availability

The data used to support the findings of this study are available from the corresponding author upon request.

#### Conflicts of Interest

The authors declare that they have no conflicts of interest.

#### Acknowledgments

This work was financially supported by the National Natural Science Foundation of China (nos. 41475023, 41730103, and 41575030) and the National Key Research

and Development Program of China (nos. 2016YFC0303900 and 2017YFC0209700).

#### References

- [1] B. Franco, W. Bader, G. C. Toon et al., "Retrieval of ethane from ground-based FTIR solar spectra using improved spectroscopy: recent burden increase above Jungfraujoch," *Journal of Quantitative Spectroscopy and Radiative Transfer*, vol. 160, pp. 36–49, 2015.
- [2] K. R. Parameswaran, D. I. Rosen, M. G. Allen, A. M. Ganz, and T. H. Risby, "Off-axis integrated cavity output spectroscopy with a mid-infrared interband cascade laser for real-time breath ethane measurements," *Applied Optics*, vol. 48, pp. B73–B79, 2009.
- [3] M. Jahjah, W. Ren, P. Stefański et al., "A compact QCL based methane and nitrous oxide sensor for environmental and medical applications," *Analyst*, vol. 139, pp. 2065–2069, 2014.
- [4] L. Tao, K. Sun, M. A. Khan, D. J. Miller, and M. A. Zondlo, "Compact and portable open-path sensor for simultaneous measurements of atmospheric  $N_2O$  and CO using a quantum cascade laser," *Optics Express*, vol. 20, no. 27, pp. 28106–28118, 2012.
- [5] A. G. Bell, "On the production and reproduction of sound by light," *American Journal of Science*, vol. 20, pp. 305–324, 1880.
- [6] C. K. N. Patel, "Laser photoacoustic spectroscopy helps fight terrorism: high sensitivity detection of chemical Warfare Agent and explosives," *European Physical Journal Special Topics*, vol. 153, no. 1, pp. 1–18, 2008.
- [7] C. Haisch, P. Menzenbach, H. Bladt, and R. Niessner, "A wide spectral range photoacoustic aerosol absorption spectrometer," *Analytical Chemistry*, vol. 84, no. 21, pp. 8941–8945, 2012.
- [8] W. Zhao, X. Gao, W. Chen et al., "Wavelength modulated off-axis integrated cavity output spectroscopy in the near infrared," *Applied Physics B*, vol. 86, no. 2, pp. 353–359, 2007.
- [9] J. J. Scherer, J. B. Paul, A. O'Keefe, and R. J. Saykally, "Cavity ringdown laser absorption spectroscopy: history, development, and application to pulsed molecular beams," *Chemical Reviews*, vol. 97, no. 1, pp. 25–51, 1997.
- [10] K. Liu, L. Wang, T. Tan et al., "Highly sensitive detection of methane by near-infrared laser absorption spectroscopy using a compact dense-pattern multipass cell," *Sensors and Actuators B: Chemical*, vol. 220, pp. 1000–1005, 2015.
- [11] R. F. Curl, F. Capasso, C. Gmachl et al., "Quantum cascade lasers in chemical physics," *Chemical Physics Letters*, vol. 487, no. 1–3, pp. 1–18, 2010.
- [12] K. Liu, J. Mei, W. Zhang, W. Chen, and X. Gao, "Multi-resonator photoacoustic spectroscopy," *Sensors and Actuators B: Chemical*, vol. 251, pp. 632–636, 2017.
- [13] T. Kuusela and J. Kauppinen, "Photoacoustic gas analysis using interferometric cantilever microphone," *Applied Spectroscopy Reviews*, vol. 42, pp. 443–474, 2007.
- [14] K. Liu, X. Guo, H. Yi, W. Chen, W. Zhang, and X. Gao, "Off-beam quartz-enhanced photoacoustic spectroscopy," *Optics Letters*, vol. 34, no. 10, pp. 1594–1596, 2009.
- [15] W. Ye, C. Li, C. Zheng et al., "Mid-infrared dual-gas sensor for simultaneous detection of methane and ethane using a single continuous-wave interband cascade laser," *Optics Express*, vol. 24, no. 15, pp. 16973–16985, 2016.
- [16] M. Hepp and M. Herman, "Vibration-rotation bands in ethane," *Molecular Physics*, vol. 98, no. 1, pp. 57–61, 2000.

- [17] L. G. Smith, "The infrared spectrum of  $C_2H_6$ ," *Journal of Chemical Physics*, vol. 17, no. 2, pp. 139–167, 1949.
- [18] A. Miklos, P. Hess, and Z. Bozoki, "Application of acoustic resonators in photoacoustic trace gas analysis and metrology," *Review of Scientific Instruments*, vol. 72, no. 4, pp. 1937–1955, 2001.

